Draft version February 25, 2021
Typeset using LaTeX **twocolumn** style in AASTeX63

A concordance scenario for the observation of a neutrino from the Tidal Disruption Event AT2019dsg

Walter Winter[1] and Cecilia Lunardini[2]

[1] *Deutsches Elektronen-Synchrotron (DESY), Platanenallee 6, D-15738 Zeuthen, Germany*
[2] *Department of Physics, Arizona State University, 450 E. Tyler Mall, Tempe, AZ 85287-1504 USA*

ABSTRACT

We introduce a phenomenological concordance scenario with a relativistic jet for the Tidal Disruption Event (TDE) AT2019dsg, which has been proposed as source of the astrophysical neutrino event IceCube-191001A. Noting that AT2019dsg is one of the brightest (and few) TDEs observed in X-rays, we connect the neutrino production with the X-rays: an expanding cocoon causes the progressive obscuration of the X-rays emitted by the accretion disk, while at the same time it provides a sufficiently intense external target of back-scattered X-rays for photo-pion production off protons. We also describe the late-term emission of the neutrino (about 150 days after the peak), by scaling the production radius with the black body radius. Our energetics and assumptions for the jet and the cocoon are compatible with expectations from numerical simulations of TDEs. We predict 0.26 neutrino events in the right energy range in IceCube.

Keywords: Neutrino astronomy (1100), Tidal disruption (1696), Relativistic jets (1390).

1. INTRODUCTION

A Tidal Disruption Event (TDE) is the process in which a star is torn apart by the tidal forces of a supermassive black hole. About 50% of the star's mass is eventually accreted by the black hole, generating a flare, which, in extreme cases of very high (super-Eddington) mass accretion rates, can result in a relativistic jet (Hills 1975; Rees 1988; Lacy et al. 1982; Phinney 1989). At least three jetted TDEs have been observed to date (Burrows et al. 2011; Cenko et al. 2012; Brown et al. 2015). TDEs have been proposed as sources of ultra-high energy cosmic rays (Farrar & Gruzinov 2009; Farrar & Piran 2014), and recently they were very actively discussed as sources of high energy astrophysical neutrinos (Wang et al. 2011; Wang & Liu 2016; Dai & Fang 2016; Senno et al. 2016; Lunardini & Winter 2017; Guépin et al. 2018; Biehl et al. 2018), especially in the context of TDEs with relativistic jets. Recent stacking searches indicate that the contribution to the diffuse extragalactic neutrino flux is limited to about 1% and 26% for jetted and non-jetted TDEs, respectively (Stein 2020).

The first likely association of a neutrino with a TDE was announced in Stein et al. (2020). The neutrino is the IceCube track-like neutrino event IceCube-191001A (IceCube Collaboration 2019), for which a dedicated multi-messenger follow up program revealed the TDE named AT2019dsg as a candidate source, with a p-value of 0.2% to 0.5% of random association (Stein et al. 2020), corresponding to $\sim 3\,\sigma$. AT2019dsg is located at redshift $z \simeq 0.05$, or luminosity distance $d_L \simeq 230$ Mpc. It was discovered in the Optical-UV bands by the Zwicky Transient Facility (ZTF) on 2019/04/09 (van Velzen et al. 2020), and it reached its luminosity peak in this band at $t_{\rm peak} = 58603$ MJD (2019/04/30). Several follow up observations were conducted in the optical-UV (van Velzen et al. 2020), radio (Perez-Torres et al. 2019; Sfaradi et al. 2019; Stein et al. 2020) and X-ray (Pasham et al. 2019b; Stein et al. 2020; Pasham et al. 2019a) bands, the latter starting at $t - t_{\rm peak} = 17$ days. IceCube-191001A followed the peak by $t - t_{\rm peak} = 154$ days and had a most likely energy $E \simeq 0.2\,$PeV, see IceCube Collaboration (2019) and links therein.

The picture that emerged from the observations (sketched in Fig. 1) shows a several months-long flare, with black body spectra observed in both the optical-UV (temperature $T_{\rm BB} = 38900\,$K, photospheric radius $R_{\rm BB} \simeq 5\,10^{14}$cm) and X-ray ($T_X \sim 0.06$ keV,

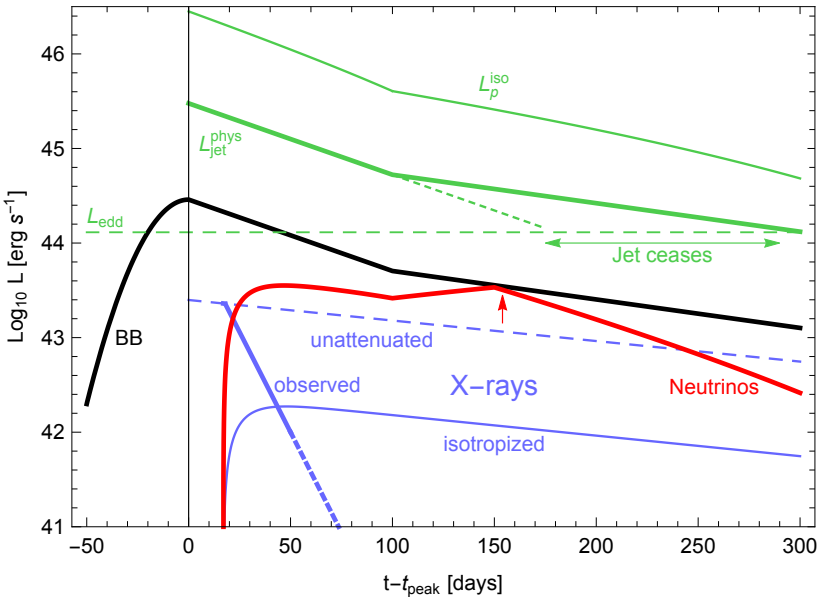

Figure 1. Time evolution of different luminosities in the jetted TDE model (labels on the curves, see text for definitions). The neutrino luminosity is a result of our work, whereas the other curves are input quantities of the model. All shown luminosities are isotropic-equivalent, and refer to the source/engine frame, except for $L_{\rm Edd}$ and $L_{\rm jet}^{\rm phys}$. The vertical arrow marks the arrival time of the observed neutrino event.

$R_X \sim 3-7\ 10^{11}$ cm) bands, and luminosities exponentially decaying over an (initial) time scale of 57.5 days and 10.3 days starting at $L_{\rm BB} = 2.88 \cdot 10^{44}\,{\rm erg\,s^{-1}}$ and $L_X \sim 2.5\ 10^{43}$ erg s^{-1}, respectively; see Fig. 1 (thick black and blue curves). The quoted X-ray luminosity is for an energy window $[0.3-8]$ keV, whereas an X-ray luminosity $L_X \sim 4\ 10^{44}$ erg s^{-1} was found in Pasham et al. (2019a) in the energy window $[0.1-10]$ keV.

Instead, the luminosity in radio emission was approximately constant over a nearly 90 days period, with increasing radius of emission $R_{\rm radio} = \mathcal{O}(10^{16})$ cm (Stein et al. 2020). The radio emission has been interpreted as an indication for a mildly relativistic outflow present over the timescale of the neutrino event. Furthermore optical polarimetry observations of this TDE cannot be uniquely interpreted, and may provide some hint for a relativistic jet (Lee et al. 2020). A further noteworthy element is that out of the 17 TDEs in the ZTF sample only four were found to have a counterpart in X-rays; of these, AT2019dsg was the one with the highest *sustained* (over several days) X-ray luminosity.

In this letter, we propose a coherent, "concordance" framework of a (dark or hidden) jetted TDE, that describes the neutrino energy and arrival time – where the latter is somewhat a challenge, considering the overall decreasing trend of the multi-messenger luminosities, see Fig. 1 (solid black and blue curves).

2. A JET CONCORDANCE MODEL

A star (of mass m) is disrupted by a supermassive black hole (SMBH, mass M) if (i) it falls within a distance less than the tidal radius:

$$r_t \simeq 9\,10^{12}\,{\rm cm}\,\left(\frac{M}{10^6\ M_\odot}\right)^{1/3}\frac{R}{R_\odot}\left(\frac{m}{M_\odot}\right)^{-1/3} \qquad (1)$$

and (ii) the tidal radius exceeds the SMBH Schwarzschild radius, $R_s = (2MG)/c^2 \simeq 3\,10^{11}\,{\rm cm}\,\big(M/(10^6\ M_\odot)\big)$ – as otherwise the star is swallowed by the black hole as a whole. The latter condition results in a upper bound on the SMBH mass, for which a conservative estimate gives $M \lesssim 2\,10^7\ M_\odot$ (Kochanek 2016). When modeling a TDE emission, an upper bound on the total energy is given by the rest energy of the disrupted star, $E_{\rm max} \sim M_\odot\ c^2 \simeq 1.8 \times 10^{54}$ erg for a solar-mass star. A useful benchmark parameter is the SMBH Eddington luminosity: $L_{\rm Edd} \simeq 1.3\ 10^{44}\ {\rm erg/s}\,\big(M/(10^6\ M_\odot)\big)$.

The Blandford-Znajek mechanism (Blandford & Znajek 1977) suggests that a weak initial magnetic field in the accretion disk in combination with a high black hole spin can lead to the formation of a jet. Numerical simulations of TDEs that are based on general relativistic radiation magnetohydrodynamics confirm this hypothesis; see, in particular, the unified model by Dai et al. (2018), where a relatively high spin and $M = 5\,10^6\ M_\odot$ were used. This simulation obtains an average mass accretion rate (at near-peak times) $\dot{M} \sim 10^2 L_{\rm Edd}$ (see also De Colle et al. (2012); Guillochon & Ramirez-Ruiz

(2013)), of which $\sim$ 20% and $\sim$ 3% go into the jet and the bolometric luminosity, respectively (a remaining 20% powers the outflow). These fractions result in a moderately super-Eddington jet, and a total radiative emission near the Eddington limit (assuming the results of Dai et al. (2018) can be rescaled for black holes of different masses):

$$L_{\rm jet}^{\rm phys} \simeq 20\, L_{\rm Edd} \simeq 3\ 10^{45}\ \frac{\rm erg}{\rm s} \left(\frac{M}{10^6\ M_\odot}\right); \quad (2)$$

$$L_{\rm bol} \simeq 3 L_{\rm Edd} \simeq 4\ 10^{44}\ \frac{\rm erg}{\rm s} \left(\frac{M}{10^6\ M_\odot}\right) . \quad (3)$$

In Dai et al. (2018), the density profile of the accretion disk was modeled, indicating that that the typical size of the optically thick region is

$$R_{\rm BB} \simeq 10^3\, R_S \simeq 3\, 10^{14}\, {\rm cm} \left(\frac{M}{10^6\ M_\odot}\right) . \quad (4)$$

The velocity profile of the gas indicated increasingly fast outflows in regions of decreasing density (away from the plane of the accretion disk and closer to the jet), with speeds reaching $v \simeq 0.5$ c.

From a comparison with the measured parameters of AT2019dsg, an overall consistency appears. We note in particular the good agreement of the blackbody luminosity and radius with Eqs. (3) and (4), which indicate a black hole mass $M \simeq 10^6\ M_\odot$ for AT2019dsg.

Moving now to describing the long term evolution ($t - t_{\rm peak} \gtrsim 10$ days) of a TDE signal, we note that no detailed numerical modeling exists, so far. Therefore, this part of the signal is more open to speculation and variety of interpretation. Here we adopt $L_{\rm BB}$ as a quantity of particular relevance, as it is probably a direct indicator of the accretion disk formed by the debris of the disrupted star. We model the time evolution of $L_{\rm BB}$ following van Velzen et al. (2020), with a change from faster to slower cooling at $t - t_{\rm peak} \gtrsim 100$ days (see Fig. 1), comparable to their power law model.

We propose a jetted TDE scenario following Lunardini & Winter (2017). In the remainder of this section, the main features, assumptions and inputs are described:

(i) Jet variability, Lorentz factor and physical energy. For the jet, a bulk Lorentz factor $\Gamma \sim \mathcal{O}(10)$ is a natural value, inspired by AGN observations (e.g. Chai et al. (2012)) and consistent with the best known jetted TDE, Swift J1644+57 (Burrows et al. 2011). We take $\Gamma = 7$, and assume a viewing angle zero, therefore the Doppler factor is $D = 2\,\Gamma \simeq 14$; these values are centered around the usual assumption of a boost factor of about 10. Matter propagating in the jet has density and velocity inhomogeneities, leading to collisions of plasma shells at the collision radius R_C where internal shocks form, and proton acceleration and subsequent neutrino production via proton-photon scattering occurs. The inhomogeneities are characterized by the variability time scale of the jet, t_v, for which the Schwarzschild time is a plausible lower limit: $t_v \gtrsim \tau_s \sim 2\pi R_s/c \simeq 63\,{\rm s}\ \left(M/(10^6\ M_\odot)\right)$. A comparable value, $t_v \simeq 100$ s, was favored by the Swift J1644+57 data (Burrows et al. 2011), and is used in this letter. Using the estimates above for Γ and t_v, one obtains a typical $R_C \sim 2\,\Gamma^2\, t_v \gtrsim 2\Gamma^2\, \tau_S \sim$ few $\times\, 10^{14}$ cm. Note how this value is comparable to $R_{\rm BB}$, Eq. (4).

For the physical energy of the jet, we assume $L_{\rm jet}^{\rm phys} = 3\, 10^{45}\, {\rm erg\, s^{-1}} \simeq 20\, L_{\rm Edd}$ at peak time, in consistency with Eq. (2). We also assume that $L_{\rm jet}^{\rm phys}$ evolves with time proportionally to $L_{\rm BB}$ until when $L_{\rm jet}^{\rm phys}$ drops below $L_{\rm Edd}$ and the jet is expected to cease (Rees 1988). The time of jet cessation depends on the (uncertain) evolution of $R_{\rm BB}$, and can take place at $\sim$170 to 300 days post-peak (see Fig. 1) – which is in any case after the time of the neutrino detection – ; we apply an exponential cutoff to the proton luminosity there. It can be estimated that over this time-scale, a total emitted energy $\lesssim 3\%\ M_\odot$ is needed to power the jet. We assume that electromagnetic signatures of the jet cannot be seen due to absorption, similarly to the case of X-rays (discussed below).

(ii) Collision radius. The long delay of the neutrino detection with respect to $t_{\rm peak}$ suggests little or no decrease of the neutrino luminosity over more than 100 days. To reproduce this feature, we introduce as a new element a time-decreasing collision radius R_C. In particular, inspired by the numerical similarity $R_C \sim R_{\rm BB}$ at peak time, we assume that R_C follows the observed evolution of $R_{\rm BB}$ (van Velzen et al. 2020):

$$\frac{R_C}{10^{14}\,{\rm cm}} \simeq \begin{cases} 5.0\, \exp\left(-\frac{t-t_{\rm peak}}{109\,{\rm d}}\right) & , t - t_{\rm peak} \leq 150\,{\rm d} \\ 1.3 & , t - t_{\rm peak} > 150\,{\rm d}\,. \end{cases} \quad (5)$$

Generally, a time-decreasing R_C can be justified in the context of the overall decline of the power of the jet, which might result e.g., in decreasing Γ. We note that the estimate $R_C \sim 2\,\Gamma^2\, t_v$ does not literally hold in multi-zone collision models, but rather a more physical description of the collision radius should be done in terms of the distance between the plasma shells and their width, see Bustamante et al. (2017) for a in-depth discussion. Since the pion production efficiency scales $\propto R_C^{-2}$, the drop in R_C will enhance the late-term neutrino production.

(iii) Target photons. Another key element of our model is that the background photons necessary for the photo-pion production originate *externally* to the

jet, as X-rays that are emitted from the inner accretion disk (at $R \sim R_X$) and are then back-scattered into the jet funnel. This assumption is attractive because it links the neutrino production to AT2019dsg being particularly bright in X-rays. The description also naturally fits the neutrino energy, as the target photon energy to produce PeV neutrinos can be estimated (for external photons boosted into the jet frame) as $E_X/\mathrm{keV} \simeq 0.025\,(E_\nu/\mathrm{PeV})^{-1}$. Therefore, for the jetted TDE scenario with external radiation, X-rays with the observed temperature are the ideal target.

The observed exponential decline of L_X suggests that a time-dependent absorption effect might be at play. Hence, we consider a scenario where an expanding outflow obscures the X-rays. For an expansion speed $v \simeq 0.1\,c$ – which is conservative, larger values are expected closer to the jet, see Dai et al. (2018) – we find that, over the characteristic X-ray decline time of ~ 10 days, the cocoon expands out to a distance $\simeq 3\,10^{15}$ cm, which can serve as an estimate for the absorption radius $R_{\rm abs}$. A comparable value of $R_{\rm abs}$ is obtained using the Thomson scattering cross section and the mass density profile in Dai et al. (2018), therefore there is basic consistency with theoretical models. Considering that $R_{\rm abs}$ exceeds the initial value of $R_{\rm C}$ by nearly an order of magnitude, it is realistic to expect that a $\sim 10\%$ fraction of the X-ray photons will be absorbed/reprocessed over the length scale $R_{\rm C} \sim R_{\rm BB}$. The scattered photons will then serve as an external target photon field of isotropized X-rays, leading to Doppler-boosted (by a factor D^2, leading to enhanced pion production) target photon density similar to external photons serving as targets in AGN, see *e.g.* Murase et al. (2014), whose description we follow here.

To implement this scenario quantitatively, we model the unattenuated X-rays luminosity according to simulations for TDEs with slim disks, e.g. Wen et al. (2020), which show that the X-ray luminosity does not follow the mass fallback rate, but stays nearly constant up to the time of flare cessation (the mass accretion rate becomes sub-Eddington), see Fig. 1. In Wen et al. (2020) an exponential drop over a time scale of 200 days post peak is found for the SMBH mass used here, which we incorporate into our model. We furthermore assume that 10% of the X-rays isotropize and build up on the attenuation timescale (thin solid blue curve in Fig. 1), with the same energy spectrum as the unattenuated parent photon flux (which is plausible considering the relatively low rate or photon re-processing). Note that this radiation will not be observable, so any late-term X-rays bounds only apply to the thick blue curve in Fig. 1.

(iv) Hadronic content of the jet. Protons are assumed to be accelerated at the collision radius R_C by internal shocks to a power law spectrum $\propto E_p'^{-2}$ (primed indices refer to the shock frame) with a maximal energy determined by balancing the acceleration rate $t_{\rm acc}'^{-1} = \eta c/R_L'$ (with moderate $\eta = 0.01$ and R_L' the Larmor radius of the proton) with the synchrotron loss and an dynamical rates (Hillas criterium). As the interactions occur in the optically thin (to $p\gamma$ interactions) regime, the requirements for proton acceleration are moderate. The (isotropic-equivalent) proton luminosity is given by $L_p^{\rm iso} \simeq (2\,\Gamma^2)\,\varepsilon\,L_{\rm jet}^{\rm phys}$, see Fig. 1, where $(2\,\Gamma^2)$ is the beaming factor and ε is the transfer efficiency from jet kinetic energy into non-thermal radiation dominated by baryons. We take $\varepsilon \simeq 0.1$, which is well within the range of typical values for Gamma-Ray Burst internal shock scenarios, see *e.g.* Pe'er (2015); Sari & Piran (1997); Kino et al. (2004); Bustamante et al. (2017); Rudolph et al. (2020).

(v) Magnetic field and other assumptions. We assume that the magnetic field energy density takes a fraction of 10% of the proton energy density (corresponding to 1% of the jet kinetic energy), which leads to a magnetic field $B' \simeq 90\,\mathrm{G}$. The neutrino mixing angles are taken from from NuFIT 4.1 (2019) (Esteban et al. 2019). Note that in our model, the information from radio data are not directly relevant for the neutrino production, mainly because $R_{\rm radio} \gg R_C$.

3. RESULTS

Our numerical treatment closely follows Lunardini & Winter (2017), with the time evolution of the spectra being calculated in discrete steps of 1 day width. The result for the time evolution of the neutrino luminosity, L_ν, is shown in Fig. 1. Its initial rise naturally follows the rise of the isotropized target X-ray flux, whereas at later times the evolution is mostly determined by the competition of the decreasing proton injection and target photon densities (driving a decrease of the neutrino flux) and the decreasing production radius R_C making the production region more compact (enhancing the neutrino flux). As a consequence of this interplay, the neutrino luminosity has two maxima, where the probability of neutrino detection is highest, one at $t - t_{\rm peak} \sim$ 30-70 days and the other at $t - t_{\rm peak} \sim$ 130-170 days. The late time luminosity revival could contribute to explaining the observed detection of one neutrino at $t - t_{\rm peak} = 154$ days. Eventually, after the revival, L_ν undergoes a sharp drop from the jet cessation or the R_C stagnation in Eq. (5). We note that the ratio of neutrino and proton luminosities is $\sim 10^{-3} - 10^{-2}$, which is natural for the optically thin regime for $p\gamma$ interactions.

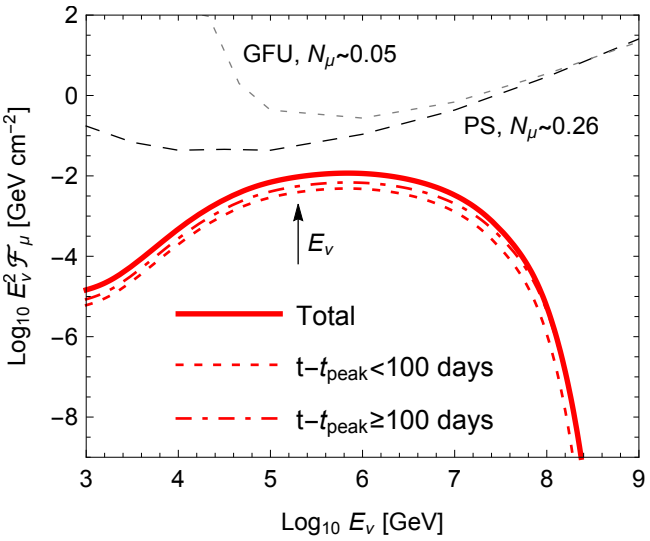

Figure 2. Predicted integrated muon neutrino and anti-neutrino fluence (including flavor mixing) for the jetted TDE model. In comparison, the differential limits and predicted event rates using the gamma-ray follow-up (GFU, Blaufuss et al. (2020)) and point source (PS, Aartsen et al. (2014)) effective areas for the declination of AT2019dsg are shown; the likely neutrino energy is taken from Stein et al. (2020). Here the differential limit is given by $E_\nu^2 \mathcal{F}_\mu^{\rm DL} = E_\nu/(A_{\rm eff}(E_\nu)\ln 10)$, which implies that following the differential limit curve precisely for one order of magnitude in energy yields one neutrino event.

Fig. 2 shows the predicted neutrino fluence, $\mathcal{F}_\mu$, as well as two differential limits on the same quantity, for comparison. Compared to other cases of proton scattering on thermal X-rays, the neutrino energy spectrum is relatively wide here due to multi-pion processes dominating the neutrino production (see, e.g., Hümmer et al. (2010) for a similar case). The most likely value of the neutrino energy ($E_\nu \sim 0.2$ PeV, with a large uncertainty allowing up to one order of magnitude larger values), falls near the maximum of the fluence.

The total, time-integrated number of events predicted in IceCube depends on the effective area used. We find $N_\nu \simeq 0.26$ when using the point source effective area, which applies to a specific, pre-identified source. The number is $N_\nu \simeq 0.05$ for the GFU effective area (see caption of Fig. 2), which includes the probability that the alert system is triggered. Note that significantly less than one event per source is expected from the Eddington bias (Strotjohann et al. 2019). From Fig. 2, we also observe that the early- and late-term contributions to the total fluence are comparable, which implies that a neutrino detection ∼150 days after the peak is plausible.

4. SUMMARY AND DISCUSSION

We have described the observation of a neutrino coincident with the tidal disruption event AT2019dsg in a jetted TDE model. In our interpretation, the unusually high X-ray luminosity of AT2019dsg is the reason for the efficient neutrino production, which implies that X-ray-bright TDEs might also be neutrino-bright. We have also shown that the late time of the neutrino signal (about 150 days after the optical peak) is not a coincidence if the neutrino production radius scales with the black body radius. Energetics are compatible with unified TDE numerical models.

Compared to the best known jetted TDEs, Swift J1644+57, AT2019dsg is very different: it is $\sim 10^3$ times less powerful (from the observer's point of view) in X-rays, and its X-ray spectrum is thermal, in contrast with the non-thermal spectrum of Swift J1644+57; therefore, the existence of a jet in AT2019dsg might be less obvious. We have nevertheless demonstrated that such jet is an option to naturally explain the observed coincident neutrino, its energy and time of arrival. Note that data from optical polarimetry of AT2019dsg may provide evidence for a relativistic jet (Lee et al. 2020).

If AT2019dsg and Swift J1644+57 are both jetted TDEs, then one will have to conclude that the phenomenology of TDEs is very diverse. New dedicated studies will be needed to explain this variety in terms of parameters such as the black hole mass and spin, the type of disrupted star, the type of star-black hole approach trajectory, etc. The diversity will then impact the estimate of the diffuse flux of neutrinos from TDEs. Our preliminary estimates show that AT2019dsg-like TDEs could contribute to the total neutrino flux observed at IceCube at the per-cent level.

We conclude that TDEs are a promising class of neutrino emitters. While we have presented only one model in this letter, other possibilities are conceivable, such as the interaction of an isotropic outflow with UV photons (Stein et al. 2020), a precessing jet pointing in our direction at late times, or the interaction of an outflow with target matter far out. We have however emphasized the connection to the X-ray observation and the parameters matching a unified TDE model from numerical simulations, which have lead to our concordance model.

Acknowledgments. We would like to thank Anna Franckowiak, Marek Kowalski, Robert Stein, and Andrew Taylor for useful discussions. This work has been supported by the European Research Council (ERC) under the European Unions Horizon 2020 research and innovation programme (Grant No. 646623), and by the US National Science Foundation grant number PHY-1613708.

REFERENCES

Aartsen, M. G., et al. 2014, Astrophys. J., 796, 109, doi: 10.1088/0004-637X/796/2/109

Biehl, D., Boncioli, D., Lunardini, C., & Winter, W. 2018, Sci. Rep., 8, 10828, doi: 10.1038/s41598-018-29022-4

Blandford, R. D., & Znajek, R. L. 1977, MNRAS, 179, 433, doi: 10.1093/mnras/179.3.433

Blaufuss, E., Kintscher, T., Lu, L., & Tung, C. F. 2020, PoS, ICRC2019, 1021, doi: 10.22323/1.358.1021

Brown, G. C., Levan, A. J., Stanway, E. R., et al. 2015, Mon. Not. Roy. Astron. Soc., 452, 4297, doi: 10.1093/mnras/stv1520

Burrows, D. N., et al. 2011, Nature, 476, 421, doi: 10.1038/nature10374

Bustamante, M., Murase, K., Winter, W., & Heinze, J. 2017, Astrophys. J., 837, 33, doi: 10.3847/1538-4357/837/1/33

Cenko, S. B., et al. 2012, Astrophys. J., 753, 77, doi: 10.1088/0004-637X/753/1/77

Chai, B., Cao, X., & Gu, M. 2012, Astrophys. J., 759, 114, doi: 10.1088/0004-637X/759/2/114

Dai, L., & Fang, K. 2016. https://arxiv.org/abs/1612.00011

Dai, L., McKinney, J. C., Roth, N., Ramirez-Ruiz, E., & Miller, M. C. 2018, Astrophys. J., 859, L20, doi: 10.3847/2041-8213/aab429

De Colle, F., Guillochon, J., Naiman, J., & Ramirez-Ruiz, E. 2012, Astrophys. J., 760, 103, doi: 10.1088/0004-637X/760/2/103

Esteban, I., Gonzalez-Garcia, M. C., Hernandez-Cabezudo, A., Maltoni, M., & Schwetz, T. 2019, JHEP, 01, 106, doi: 10.1007/JHEP01(2019)106

Farrar, G. R., & Gruzinov, A. 2009, Astrophys. J., 693, 329, doi: 10.1088/0004-637X/693/1/329

Farrar, G. R., & Piran, T. 2014. https://arxiv.org/abs/1411.0704

Guillochon, J., & Ramirez-Ruiz, E. 2013, Astrophys. J., 767, 25, doi: 10.1088/0004-637X/798/1/64,10.1088/0004-637X/767/1/25

Guépin, C., Kotera, K., Barausse, E., Fang, K., & Murase, K. 2018, Astron. Astrophys., 616, A179, doi: 10.1051/0004-6361/201732392

Hills, J. G. 1975, Nature, 254, 295. http://dx.doi.org/10.1038/254295a0

Hümmer, S., Rüger, M., Spanier, F., & Winter, W. 2010, Astrophys. J., 721, 630, doi: 10.1088/0004-637X/721/1/630

IceCube Collaboration. 2019, GRB Coordinates Network, 25913, 1

Kino, M., Mizuta, A., & Yamada, S. 2004, Astrophys. J., 611, 1021, doi: 10.1086/422305

Kochanek, C. S. 2016, doi: 10.1093/mnras/stw1290

Lacy, J. H., Townes, C. H., & Hollenbach, D. J. 1982, Astrophys. J., 262, 120, doi: 10.1086/160402

Lee, C.-H., Hung, T., Matheson, T., et al. 2020, The Astrophysical Journal, 892, L1, doi: 10.3847/2041-8213/ab7cd3

Lunardini, C., & Winter, W. 2017, Phys. Rev., D95, 123001, doi: 10.1103/PhysRevD.95.123001

Murase, K., Inoue, Y., & Dermer, C. D. 2014, Phys. Rev., D90, 023007, doi: 10.1103/PhysRevD.90.023007

Pasham, D., Remillard, R., Loewenstein, M., et al. 2019a, The Astronomer's Telegram, 12825, 1

Pasham, D., Remillard, R., & Wevers, T. 2019b, The Astronomer's Telegram, 12777, 1

Pe'er, A. 2015, Adv. Astron., 2015, 907321, doi: 10.1155/2015/907321

Perez-Torres, M., Moldon, J., Mattila, S., et al. 2019, The Astronomer's Telegram, 12960, 1

Phinney, E. S. 1989, in IAU Symposium, Vol. 136, The Center of the Galaxy, ed. M. Morris, 543

Rees, M. J. 1988, Nature, 333, 523, doi: 10.1038/333523a0

Rudolph, A., Heinze, J., Fedynitch, A., & Winter, W. 2020, Astrophys. J., 893, 72, doi: 10.3847/1538-4357/ab7ea7

Sari, R., & Piran, T. 1997, Astrophys. J., 485, 270, doi: 10.1086/304428

Senno, N., Murase, K., & Meszaros, P. 2016. https://arxiv.org/abs/1612.00918

Sfaradi, I., Williams, D., Horesh, A., et al. 2019, The Astronomer's Telegram, 12798, 1

Stein, R. 2020, PoS, ICRC2019, 1016, doi: 10.22323/1.358.1016

Stein, R., et al. 2020. https://arxiv.org/abs/2005.05340

Strotjohann, N. L., Kowalski, M., & Franckowiak, A. 2019, Astron. Astrophys., 622, L9, doi: 10.1051/0004-6361/201834750

van Velzen, S., et al. 2020. https://arxiv.org/abs/2001.01409

Wang, X.-Y., & Liu, R.-Y. 2016, Phys. Rev., D93, 083005, doi: 10.1103/PhysRevD.93.083005

Wang, X.-Y., Liu, R.-Y., Dai, Z.-G., & Cheng, K. S. 2011, Phys. Rev., D84, 081301, doi: 10.1103/PhysRevD.84.081301

Wen, S., Jonker, P. G., Stone, N. C., Zabludoff, A. I., & Psaltis, D. 2020. https://arxiv.org/abs/2003.12583